

# TG-60 dosimetry parameters calculation for the $\beta$ -emitter $^{153}\text{Sm}$ brachytherapy source using MCNP

F. Taghdiri<sup>1</sup>, M. Sadeghi<sup>2\*</sup>, S.H. Hosseini<sup>1</sup>, M. Athari<sup>1</sup>

<sup>1</sup>Department of Nuclear Engineering, Science and Research Branch, Islamic Azad University, Tehran, Iran

<sup>2</sup>Agricultural, Medical and Industrial Research School, Nuclear Science and Technology Research Institute, Karaj, Iran

**Background:** The formalism recommended by Task Group 60 (TG-60) of the American Association of Physicists in Medicine (AAPM) is applicable for  $\beta$  sources. Radioactive biocompatible and biodegradable  $^{153}\text{Sm}$  glass seed without encapsulation is a  $\beta$ -emitter with a short half life and delivers a high dose rate to the tumor in the millimeter range. In this work the dosimetry parameters of the seed for brachytherapy were evaluated. **Materials and Methods:** Using MCNP4C code data, the Dosimetric parameters of AAPM TG-60 recommendations including the reference dose rate, the radial dose function and the anisotropy function were obtained. Two dimensional dose distributions were also calculated. **Results:** The dose rate at reference point was estimated to be  $9.41 \text{ cGy}\cdot\text{h}^{-1}\cdot\mu\text{Ci}^{-1}$  for  $^{153}\text{Sm}$ .  $^{153}\text{Sm}$  with its relatively low energy beta component falls off the most rapidly of the other beta emitters. The calculated data was compared with that of several beta and photon emitting seeds. **Conclusion:** The results showed the advantage of the beta emitting  $^{153}\text{Sm}$  source in comparison with the other beta emitting sources, Because of its rapid dose fall-off of beta-ray and high dose rate at the short distances of the seed. The results would be helpful in development of the radioactive implants using  $^{153}\text{Sm}$  seeds for the brachytherapy treatment. *Iran. J. Radiat. Res., 2011; 9(2): 103-108*

**Keywords:** Beta emitters,  $^{153}\text{Sm}$  seed, dosimetry, TG-60 protocol, MCNP4C code.

## INTRODUCTION

The history of beta brachytherapy is very short compared with conventional gamma brachytherapy. In intravascular brachytherapy, beta emitting sources are typically used for their short range<sup>(1, 2)</sup>.

$^{125}\text{I}$  and  $^{103}\text{Pd}$  seeds are used in permanent radioactive implants in the prostate. These seeds, however, have a metallic encapsulation and after the radioisotope decayment, the material does not interact with the tissue since it is inert<sup>(3, 4)</sup>. Considering the complicated technology

involved in the production of these metallic seeds and the indefinitely permanence of those material in the human organs after the therapy, the project of a bioactive and biodegradable material is in progress<sup>(1)</sup>. Unlike the permanent interstitial Brachytherapy, applying biodegradable material is compatible with the biological medium.

$^{153}\text{Sm}$  is a radionuclide with very interesting therapeutically features, with beta radiation of 0.640, 0.710 and 0.810 MeV, maximum energy, and 103 keV of gamma radiation, among others. Additionally, emission of 103 keV gamma ray cause to be detected by gamma camera.  $^{153}\text{Sm}$  produces in reactors by using enriched samarium ( $^{152}\text{Sm}$ ) by the  $(n, \gamma)$  reaction. This enables the production of  $^{153}\text{Sm}$  at low cost in comparison of conventional seeds. The  $^{153}\text{Sm}$  radionuclide decays by beta rays followed by gamma-rays emission, with a half life of 46 h<sup>(5, 6)</sup>. Encapsulation is not required because the seed is unreactive in water or tissue during decay time and it is absorbed after 7 months by the organ. The seed compositions make it detectable by ultrasonography. Seven months after the implant, no ecographic signal of the seeds was observed from images of ultrasonography<sup>(1)</sup>.

In previously published investigations preliminary studies for the implant of biodegradable radioactive  $^{153}\text{Sm}$  seeds in the liver<sup>(1)</sup>, brain<sup>(7, 8)</sup>, and prostate<sup>(9)</sup> have been prepared.  $^{153}\text{Sm}$  is used as compounds ( $^{153}\text{Sm}$ -EDTMP) for the relief of pain in bone without significant toxicity<sup>(10)</sup>.

### \*Corresponding author:

Dr. Mahdi Sadeghi,  
Agricultural, Medical and Industrial Research School,  
P.O. Box: 31485/498, Karaj, Iran.  
Fax: +98 261 4436395  
E-mail: msadeghi@nrcam.org

For radionuclide selection, several factors must be considered. Beta emitters such as  $^{90}\text{Sr}/^{90}\text{Y}$  and  $^{32}\text{P}$  have a long range of high-energy beta emitting (2.282 MeV and 1.710 MeV, respectively), but with the absence of accompanying  $\gamma$  emissions, they cannot be traced during therapy. On the other hand, Samarium-153 is a radiolanthanide with interesting characteristics, which has not yet been widely used.

The updated AAPM TG-43 report recommended a dosimetry protocol for interstitial brachytherapy sources <sup>(1)</sup>. TG-43 parameters are particularly for low energy photon emitters such as  $^{125}\text{I}$  and  $^{103}\text{Pd}$  and beta emitting sources were not included. The AAPM TG-60 report included intravascular brachytherapy physics and dosimetry parameters of beta emitters <sup>(12)</sup>. In this work the reference dose rate, the radial dose function and the two dimensional anisotropy functions were calculated using MCNP4C code according to the AAPM TG-60 report. The dose rates were also derived in different radial distances from the source and isodose curves.

## MATERIALS AND METHODS

$^{153}\text{Sm}$  glass seed is made of Si-Ca- $^{153}\text{Sm}$  and it consists 20% of Samarium, 30% of calcium and 50% of silicon, of cylindrical format, with dimensions of approximately  $0.3 \times 1.6$  mm, and the density of  $1.76 \text{ g/cm}^3$  <sup>(1)</sup>. Figure 1 shows the geometry of  $^{153}\text{Sm}$  seed and the coordinate system.

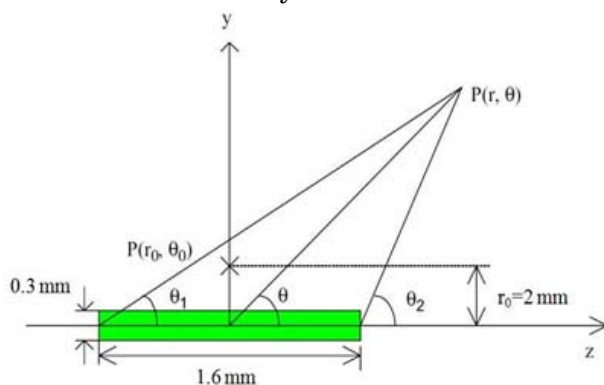


Figure 1. Scheme of the  $^{153}\text{Sm}$  seed and coordinate system according to the AAPM TG- 60.

## Monte Carlo simulation

Due to the rapid dose decrease around the beta sources, it is extremely difficult to obtain accurate dose experimentally. Therefore, Monte Carlo calculation is widely used as an alternative method to analyze the dose distribution around the radioactive seeds for therapeutic purposes. In this study MCNP4C code was used to calculate the dosimetric parameters of the  $^{153}\text{Sm}$  glass seed. Although the code had the ability to transport neutron, electron and gamma particles independently or in a couple or a triplet, the procedure should have been initiated by only one of the particles <sup>(13)</sup>.  $^{153}\text{Sm}$  emits electron and gamma particles simultaneously; therefore, separate dose rate calculations were performed and the sum was taken as the total dose rate. For electron transport, all secondary particle effects (including bremsstrahlung) were simulated together with coupled electron-photon transport. The Monte Carlo  $N$ -particle code modeled a three-dimensional geometry, and various source types such as point, volume and surface with user-defined source spectrum. For simulating dose distribution a cylindrical volume source was modeled in a spherical water phantom. The radioisotope was assumed to be uniformly distributed in the seed. Beta irradiation with 0.71, 0.64 and 0.81 MeV and gamma irradiation with 0.103 MeV were considered. The dose values in water were calculated according to the TG-60 protocol at radial distances of 0.3 to 3.5 mm and at polar angles of  $0^\circ$ – $90^\circ$  in  $10^\circ$  increments. The \*F8 tally was used to score deposited energy (MeV) in the detectors around the seed, and it was divided by the detectors mass, and then multiplied by appropriate conversion factor to obtain absorbed dose. The dose rate of the beta radiation of the  $^{153}\text{Sm}$  in rang of millimeters was compared with the gamma radiation for those distances. The seed were plotted according to MCNP4C results isodose curves.

## RESULTS AND DISCUSSION

The use of beta sources such as  $^{90}\text{Y}$ ,  $^{32}\text{P}$ ,  $^{188}\text{Re}$ , and  $^{90}\text{Sr}/^{90}\text{Y}$  in brachytherapy has several advantages over typical gamma sources. Beta emitters have short range and are easily shielded, lowering the dose for the medical staff as well as the patient. This beta brachytherapy technique can significantly decrease the radiation doses to normal tissue without decreasing radiation dose to tumor cells <sup>(14)</sup>. In the case of prostate cancer, beta emitting radionuclides can give a lower dose to the rectum and urethra than low energy photons <sup>(15)</sup>. The dose to the urethra and rectum walls from conventional brachytherapy could be more than 360 and 90 Gy, respectively <sup>(16)</sup>.

Table 1, presents the dose rate values calculated in this work using MCNP4C code. The comparison of these values with the previously published data for  $^{142}\text{Pr}$  glass seed <sup>(15)</sup> showed a good agreement. The results differences were from 1% to 5%.

**Table 1.** Monte Carlo calculated dose rate values of  $^{142}\text{Pr}$  glass seed.

Radial distance (mm)	Dose rate (cGy.h <sup>-1</sup> . $\mu\text{Ci}^{-1}$ )
	$^{142}\text{Pr}$ glass seed
1.0	6.930
1.5	3.873
2.0	2.480
2.5	1.670
3.0	1.125
3.5	0.695
4.0	0.469
5.0	0.205
6.0	0.067
7.0	0.022

Figure 2 shows the comparison of radial dose function,  $g(r)$ , of  $^{153}\text{Sm}$  and IRA- $^{103}\text{Pd}$  <sup>(4)</sup>. The radial dose function for IRA- $^{103}\text{Pd}$  was flat to about 1 cm and then decreased gradually, while the radial dose function profile for  $^{153}\text{Sm}$  fell off rapidly at about 0.2 cm. Therefore, the undesirable dose to

adjacent organs was insignificant for  $^{153}\text{Sm}$  seed.

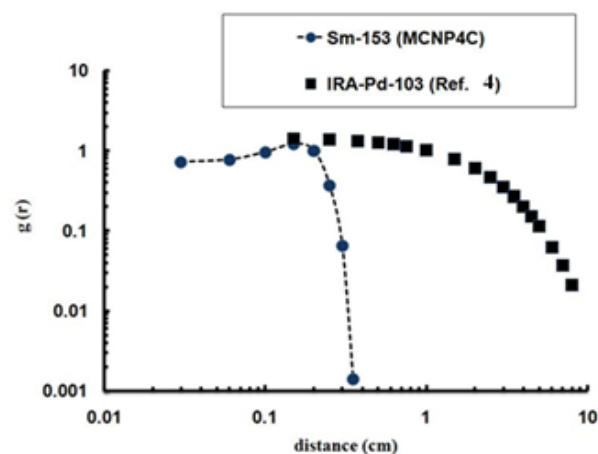


**Figure 2.** Comparison of the Monte Carlo calculated radial dose functions of the  $^{153}\text{Sm}$  and  $^{103}\text{Pd}$  seeds.

The dosimetric parameters defined in AAPM TG-60 including: reference dose rate, radial dose function and two-dimensional anisotropy function were determined using the Monte Carlo calculations. The dose at a point from the seed can be expressed as <sup>(12)</sup>,  $D(r, \theta) = D(r_0, \theta_0) [G(r, \theta)/G(r_0, \theta_0)] g(r) F(r, \theta)$  <sup>(1)</sup>

Where  $r$  is the radial distance from the source,  $\theta$  the angle between the line segment from point of interest to center of source,  $G(r, \theta)$  the geometry function resulting from spatial distribution of the radioactivity within the source,  $g(r)$  the radial dose function,  $F(r, \theta)$  the two-dimensional anisotropy function describing the dose variation and  $D(r_0, \theta_0)$  is the dose rate in water at the reference point. The reference point suggested in AAPM TG-60 is  $r_0=2$  mm and  $\theta_0=90$ . The geometry function was calculated for a line source using the f4 tally, particle fluence ( $1/\text{cm}^2$ ) in the each detector by considering the mass densities of all materials in simulation equal to zero <sup>(17)</sup>.

The Simulations were performed having  $10^8$  electron histories in water with statistical uncertainties of 0.2%, 0.6% and 5%, at 0.6, 2 and 3 mm on the transverse plane and 1% and 6% at 1 and 3 mm along the long axis.

**The reference dose rate for  $^{153}\text{Sm}$  source:**

The reference dose rate was defined at the source bisector orthogonal to source long axis at a radial distance of 2 mm and  $\theta=90^\circ$ . Table 2 shows the values of the dose rate for different distances from the center of the source. The dose rate at reference dose point D ( $r_0, \theta_0$ ) for  $^{153}\text{Sm}$  was calculated to be  $9.41 \text{ cGy.h}^{-1}.\mu\text{Ci}^{-1}$ . The value was higher than the values of 2.412, 6.0 and  $1.081 \text{ cGy.h}^{-1}.\mu\text{Ci}^{-1}$ , calculated for  $^{142}\text{Pr}$  (maximum energy of 2.162 MeV),  $^{90}\text{Sr}/^{90}\text{Y}$ , and  $^{32}\text{P}$ , respectively (15, 18, 19). Also, the  $\beta$  and  $\gamma$  radiations of  $^{153}\text{Sm}$  had shorter range over  $^{32}\text{P}$ ,  $^{142}\text{Pr}$  and  $^{90}\text{Sr}/^{90}\text{Y}$ . Figure 3 shows the radial dose profiles of  $\beta$  and  $\gamma$  dose from the  $^{153}\text{Sm}$  seed. The dose profile of  $\gamma$  decreased gradually, but the dose profile from  $\beta$  has dropped sharply. As with gamma-emitting sources, beta-emitters showed very high dose rate gradients at close distances to the source, but unlike gamma emitters, insignificant doses at larger distances. Figure 4 shows the comparison of dose rate profile of  $^{153}\text{Sm}$  calculated from the MCNP4C code and beta emitters of  $^{90}\text{Sr}/^{90}\text{Y}$  and  $^{32}\text{P}$  and  $^{142}\text{Pr}$ . The figure shows the  $^{153}\text{Sm}$  has delivered higher dose rate at very short range distance in comparison with the other beta emitters. The dose fall off rates are related to the mean (or maximum) beta energies.  $^{90}\text{Sr}/^{90}\text{Y}$  with the highest mean beta energy has the slowest dose fall off in tissue, while  $^{153}\text{Sm}$  with the lowest mean beta energy shows the most rapid dose fall off.

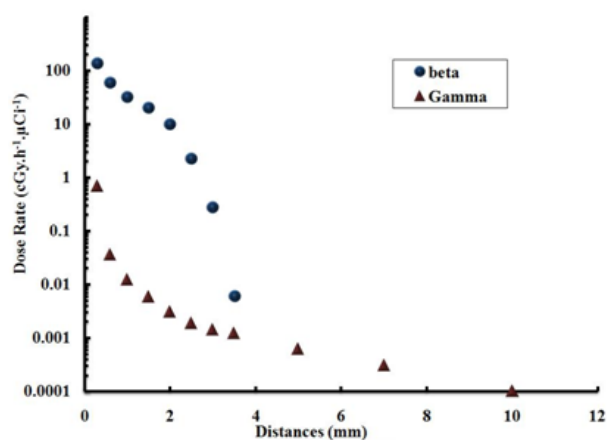


Figure 3. Dose rate profiles of  $\beta$  and  $\gamma$  radiations of the  $^{153}\text{Sm}$  source.

Table 2. Calculated dose rate for beta and gamma radiation of  $^{153}\text{Sm}$  from MCNP4C simulation.

Distance (mm)	Dose Rate ( $\text{cGy.h}^{-1}.\mu\text{Ci}^{-1}$ )	
	$\beta$	$\gamma$
0.3	130.9	0.6726
0.6	56.06	0.0251
1	30.81	0.0117
1.5	19.11	0.0057
2	9.41	0.0030
2.5	2.19	0.0018
3	0.271	0.0014
3.5	0.006	0.0012
5		0.0006
7		0.0003
10		0.0001

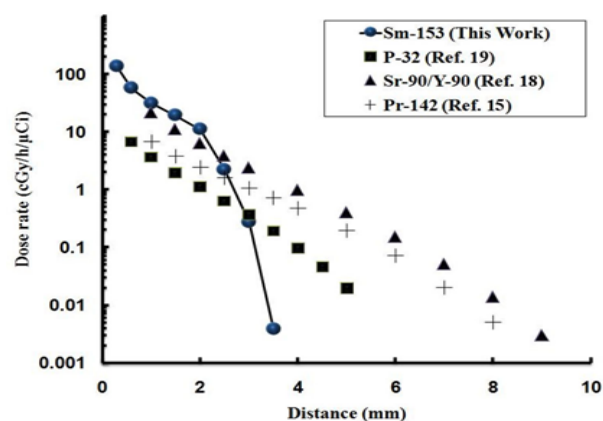


Figure 4. Comparison of dose rate profiles of various  $\beta$  emitters as a function of distance.

**Radial dose function**

The radial dose function  $g(r)$  is calculated as (11),

$$g(r) = \frac{\dot{D}(r, \theta_0) G(r_0, \theta_0)}{\dot{D}(r_0, \theta_0) G(r, \theta_0)} \quad (2)$$

In figure 5 radial dose function of  $^{153}\text{Sm}$  is compared with several beta emitters such as  $^{90}\text{Sr}/^{90}\text{Y}$  and  $^{90}\text{Y}$  (20, 21). The values of the  $^{153}\text{Sm}$  source radial dose function are calculated using MCNP4C code and presented in table 3. Due to the short range of beta particles of  $^{153}\text{Sm}$ , it has the shortest penetration compared with those of  $^{90}\text{Sr}/^{90}\text{Y}$  and  $^{90}\text{Y}$  seeds. For  $^{153}\text{Sm}$ , the dose within 2 mm is much higher than with other seeds. It can be seen that  $^{153}\text{Sm}$  has more rapid dose fall off than the  $^{90}\text{Sr}/^{90}\text{Y}$  and  $^{90}\text{Y}$  sources.



**Table 3.** MCNP4C calculated radial dose function,  $g_L(r)$ , the  $^{153}\text{Sm}$  seed.

r (mm)	g(r)
0.3	0.716
0.6	0.768
1.0	0.951
1.5	1.202
2.0	1.000
2.5	0.364
3.0	0.063
3.5	0.002

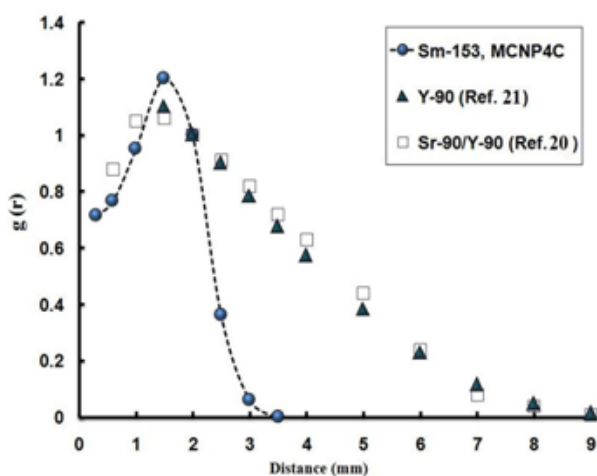


**Figure 5.** Comparison of the Monte Carlo calculated Radial dose function of the  $^{153}\text{Sm}$  source with those of the  $^{90}\text{Sr}/^{90}\text{Y}$  and  $^{90}\text{Y}$  sources.

**The anisotropy function,  $F(r,\theta)$**

The two-dimensional anisotropy function,  $F(r,\theta)$ , is defined as <sup>(11)</sup>,

$$F(r,\theta) = \frac{\dot{D}(r,\theta) G_L(r,\theta_0)}{\dot{D}(r,\theta_0) G_L(r,\theta)} \quad (3)$$

**Table 4.** The values of two-dimensional anisotropy function for the  $^{153}\text{Sm}$  seed from MCNP4C simulation.

Distance (mm)	Angle (degree)									
	0	10	20	30	40	50	60	70	80	90
0.3					0.925	0.961	0.979	0.981	0.997	1
0.6			0.792	0.877	0.924	0.948	0.966	0.993	0.999	1
1	0.605	0.621	0.691	0.769	0.829	0.898	0.936	0.965	0.989	1
1.5	0.653	0.619	0.673	0.736	0.812	0.872	0.928	0.975	0.988	1
2	0.699	0.780	0.825	0.883	0.930	0.969	0.988	0.998	0.999	1
2.5	1.621	1.531	1.520	1.513	1.434	1.338	1.217	1.107	1.025	1
3	3.924	3.273	3.030	2.796	2.373	1.886	1.547	1.245	1.091	1
3.5	42.22	28.69	25.84	21.451	15.27	9.750	5.938	2.952	1.639	1

Table 4 presents values of the two dimensional anisotropy function. The maximum value of the anisotropy function was calculated to be 42.22. This was due to the isodose profile which was elliptical as shown in figure 6. Most conventional seeds had significant cold spots at the ends of the seed due to attenuation through the seed and encapsulation at the edges, while the  $^{153}\text{Sm}$  seed dose rate increased particularly for  $r > 2$  mm.

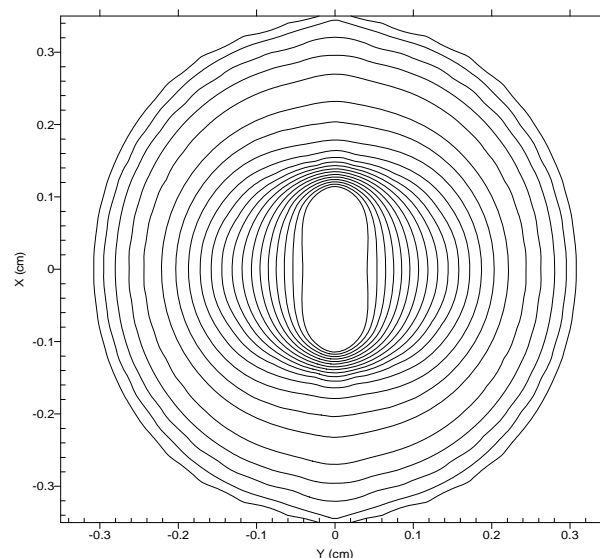


**Figure 6.** Isodose contour map around the  $^{153}\text{Sm}$  seed.

**CONCLUSION**

Dosimetric parameters, including reference dose rate, radial dose function, and two-dimensional anisotropy function of the  $^{153}\text{Sm}$  brachytherapy source have been

calculated by using the MCNP4C Monte Carlo code. These calculations were performed following the AAPM TG-60 task group recommendations and compared with the previous published data. The information has been presented in tabulated and graphical format. Dose rate in reference point at 2 mm was calculated to be  $9.41 \text{ cGy.h}^{-1}.\mu\text{Ci}^{-1}$ , which was higher than the other beta emitters. Because of short range of beta particle, damage to healthy adjacent organs was negligible. The result presented the main advantages of  $^{153}\text{Sm}$  seed in liver, brain and prostate.

## REFERENCES

1. Campos TPR, Andrade JPL, Costa IT, Silva CHT (2008) Study of the  $^{153}\text{Sm}$  seeds degradation and devaluation of the absorbed dose in rabbit's liver implants. *Progress in Nuclear Energy*, **50**: 757-766.
2. Lee SW (2003) Beta dose calculation in human arteries for various brachytherapy seed types. PhD Thesis, Texas University, USA.
3. Duggan DM and BL Johnson (2001) Dosimetry of the I-Plant Model 3500 Iodine-125 brachytherapy source. *Med Phys*, **28**: 661-670.
4. Sadeghi M, Raisali Gh, Hosseini SH, Shavar A (2008) Monte Carlo calculations and experimental measurements of dosimetric parameters of the IRA- $^{103}\text{Pd}$  brachytherapy source. *Med Phys*, **35**: 1288-1294.
5. Fani M, Vranjes S, Archimandritis SC, Potamianos S, Xanthopoulos S, Bouziotis P, Varvarigou AD (2002) Labeling of monoclonal antibodies with  $^{153}\text{Sm}$  for potential use in radioimmunotherapy. *Appl Radiat Isot*, **57**: 665-674.
6. De Lima CF and de Campos TPR (2005) Dosimetric evaluation in radiation synovectomy. *Brazilian Archives of Biology and Technology*, **48**: 153-158.
7. Silva GXO, Campos TPR, Siqueira SL, Maciel MB (2005) The surgical viability and radiobiological monitoring of brain implants of bioactive microseeds in animal model. *Brazilian Archives of Biology and Technology*, **48**: 109-115.
8. Costa IT and Campos TPR (2007) Dosimetric response of radioactive bioglass seeds implants on rabbit's brain. *Matéria Rio J*, **12**: 480-486.
9. Roberto WS, Pereira MM, Campos TPR (2003) Structure and dosimetric analysis of biodegradable glasses for prostate cancer treatment. *International Society for Artificial Organs*, **27**: 432-436.
10. Sartor O (2004) Overview of samarium Sm 153 leixidronam in the treatment of painful metastatic bone disease. *Advances in Prostate Cancer*, **6**: S3-S12.
11. Rivard MJ, Coursey BM, DeWerd LA, Hanson WF, Huq MS, Ibbott GS, Mitch MG, Nath R, Williamson JF (2004) Update of AAPM Task Group No. 43 Report: A revised AAPM protocol for brachytherapy dose calculations. *Med Phys*, **31**: 633-674.
12. Nath R, Amols H, Coffey C and Duggan D, Jani S, Li Z, Schell M, Soares C, Whiting J, Cole PE, Crocker I, Schwartz R (1999) Intravascular brachytherapy physics: Report of the AAPM Radiation Therapy Committee Task Group No. 60. *Med Phys*, **26**: 119-152.
13. Briesmeister JF (2000) MCNP—A general Monte Carlo N-particle transport code—Version 4C. Los Alamos National Laboratory Report No. LA- 13709-M.
14. Baucal M (2000) Physical aspects of endovascular brachytherapy. *Archive of Oncology*, **8**: 15-9.
15. Jung JW and Reece WD (2008) Dosimetric characterization of  $^{142}\text{Pr}$  glass seeds for brachytherapy. *Applied Radiation and Isotopes*, **66**: 441-449.
16. Wallner K, Roy J, Harrison L (1995) Dosimetry guidelines to minimize urethral and rectal morbidity following transperineal I-125 prostate brachytherapy. *Int J Radiat Oncol Biol Phys*, **32**: 465-471.
17. Rivard MJ (2001) Monte Carlo calculation of AAPM Task Group Report No.43 dosimetry parameters for the MED3631-A/M  $^{125}\text{I}$  source. *Med Phys*, **28**: 629-637.
18. Wang R and Li XA (2002) Dosimetric comparison of two  $^{90}\text{Sr}/^{90}\text{Y}$  sources for intravascular brachytherapy: An EGSnc Monte Carlo calculation. *Phys Med Biol*, **47**: 4259-4269.
19. Mourtada F, Soares CG, Horton JL (2004) A segmented  $^{32}\text{P}$  source Monte Carlo model to derive AAPM TG-60 dosimetric parameters used for intravascular brachytherapy. *Med Phys*, **31**: 602-608.
20. Massillon-JL G, Minniti R, Mitch MG, Maryanski MJ, Soares CG (2009) The use of gel dosimetry to measure the 3D dose distribution of a  $^{90}\text{Sr}/^{90}\text{Y}$  intravascular brachytherapy seed. *Phys Med Biol*, **54**: 1661-1672.
21. Patel NS, Chiu-Tsao Sou-Tung, Fan P, Ahunbay E, Ravi K, Sherman W, Quon H, Pisch J, Hung-Sheng T, Harrison LB (2001) Treatment planning dosimetric parameters for a  $^{90}\text{Y}$  coil source used in intravascular brachytherapy. *Cardiovascular Radiation Medicine*, **2**: 83-92.